First publ. in: Journal of Applied Physics ; 113 (2013), 2. - 023906

AIP | Journal of Applied Physics

Properties of magnetic vortices at elevated temperatures

Kristof M. Lebecki and Ulrich Nowak

Citation: J. Appl. Phys. **113**, 023906 (2013); doi: 10.1063/1.4774411

View online: http://dx.doi.org/10.1063/1.4774411

View Table of Contents: http://jap.aip.org/resource/1/JAPIAU/v113/i2

Published by the American Institute of Physics.

JOURNAL OF APPLIED PHYSICS 113, 023906 (2013)

Properties of magnetic vortices at elevated temperatures

Kristof M. Lebecki[a)] and Ulrich Nowak
Department of Physics, University of Konstanz, 78457 Konstanz, Germany

(Received 24 August 2012; accepted 18 December 2012; published online 10 January 2013)

Thermal properties of steady-state magnetic vortices in soft materials are numerically evaluated using the recently proposed Landau-Lifshitz-Bloch approach. Circular samples with permalloy-like parameters are simulated. Relevant properties of the vortex core, as its radius, the magnetization drop in its center, and the radius of this magnetization drop are extracted. The dependence of the vortex core radius on temperature agrees well with the theoretical predictions, if only temperature-dependent parameters are taken into account. A new effect is found, which we call magnetization squeezing, resulting from the thermodynamic nature of the Landau-Lifshitz-Bloch approach. Our results show, however, that this squeezing in vortices is a rather weak effect in permalloy. © *2013 American Institute of Physics*. [http://dx.doi.org/10.1063/1.4774411]

I. INTRODUCTION

Magnetic vortices are objects of rotational symmetry composed of a small-sized core, where the magnetization is pointing out of the film plane, surrounded by in-plane magnetization—see Fig. 1. They have been known already for a long time, see, for example, Ref. 1, but only recently they have attracted remarkable attention due to their potential applications. First, they are stable objects that are suitable as basic building blocks for memory storage applications.[2] A second application suggested recently is related to nanooscillators working in the sub-gigahertz regime.[3]

Another subject attracting interest recently is the temperature properties of magnetic nanostructures. This interest is stimulated by the idea of heat assisted magnetic recording[4] and all-optical magnetic recording.[5] The influence of temperature on the properties of a domain wall in materials with large anisotropy has already been reported.[6] However, to effectively design devices, basing on vortices knowledge of their temperature properties is necessary. As the bulk of experiments on vortices takes place in soft samples—usually this is permalloy(see, e.g., Refs. 2 and 3)—we focus our attention on this material. Especially, we consider closely center of the vortex—the vortex core. In this paper, we report on its dependence and behavior in temperatures up to 99% of the Curie temperature.

II. MODEL AND METHODS

We follow a temperature-dependent numerical micromagnetic approach, where the Landau-Lifshitz-Bloch (LLB) equation is used.[7] The LLB equation is an extension of the well-known Landau-Lifshitz-Gilbert (LLG) equation of motion,[8] for a case of non-zero temperature, $T \geq 0$,

$$\dot{\mathbf{M}} = -\bar{\gamma}\,\mathbf{M}\times\mathbf{H}_{\rm eff} + \bar{\gamma}\,\alpha_{\parallel}\frac{M_{\rm s}}{M^2}(\mathbf{M}\cdot\mathbf{H}_{\rm eff})\mathbf{M} - \bar{\gamma}\,\alpha_{\perp}\frac{M_{\rm s}}{M^2}\mathbf{M}\times(\mathbf{M}\times\mathbf{H}_{\rm eff}). \quad (1)$$

Here $\bar{\gamma}$ is the gyromagnetic ratio, $\mathbf{M}$ is the magnetization, $\mathbf{H}_{\rm eff}$ is the effective field (see Eq. (2)), $\alpha_{\parallel}$ and $\alpha_{\perp}$ are, respectively, longitudinal and transversal damping coefficients (see Eq. (3)), $M_{\rm s}$ is the saturation magnetization (at $T=0$) and $M = |\mathbf{M}|$. The effective field has a similar form as in the case of the LLG approach with an additional term that prevents too large deviations of the magnetization magnitude from its equilibrium magnetization, $M_{\rm e}(T)$,

$$\mathbf{H}_{\rm eff} = \mathbf{H}_{\rm d} + \frac{2A}{\mu_0 M_{\rm e}^2}\nabla^2\mathbf{M} - \left(\frac{M^2}{M_{\rm e}^2} - 1\right)\frac{\mathbf{M}}{2\chi_{\parallel}}, \quad (2)$$

where $\mathbf{H}_{\rm d}$ is the demagnetization field, A is exchange constant, μ_0 is vacuum permeability, and $\chi_{\parallel}$ is the longitudinal susceptibility. We have ignored here anisotropy effects as we focus our attention on permalloy (Py). Note that $M_{\rm e}(0) = M_{\rm s}$. The LLB longitudinal and transversal damping coefficients are given by

$$\alpha_{\parallel} = \alpha\, 2T/3T_{\rm C}, \quad \alpha_{\perp} = \alpha(1 - T/3T_{\rm C}), \quad (3)$$

where α is the Gilbert damping constant (for $T=0$) and $T_{\rm C}$ is the Curie temperature.[9] Contrary to the zero-temperature LLG equation, in the LLB approach, the material parameters are actually temperature dependent functions $M_{\rm e}(T)$, $A(T)$, and $\chi_{\parallel}(T)$. Another important feature of the LLB equation is the non-constant magnetization magnitude, $M(\mathbf{r}, t)$, that can vary in space and in time. This process is monitored by the last term in Eq. (2). Thus, for small temperatures, where $\chi_{\parallel}$ is small M tends to $M_{\rm e}(T)$, while for larger temperatures, where $\chi_{\parallel}$ increases (diverging at $T_{\rm C}$) local differences between M and $M_{\rm e}(T)$ can be larger. This happens, for example, inside a domain wall.[6]

Our code is an extension to the well-known simulation package, OOMMF.[10] In our implementation, we have followed Ref. 11. One difference between our implementation and that of Kazantseva *et al.*[11] is omitting the thermal stochastic field, because we are solely interested in steady state calculations, similarly as in our previous report.[12]

The sample we have modeled is a thin ferromagnetic disk with radius $r = 100$ nm and a thickness $t = 20$ nm.

a)Electronic mail: Kristof.Lebecki@uni-konstanz.de.

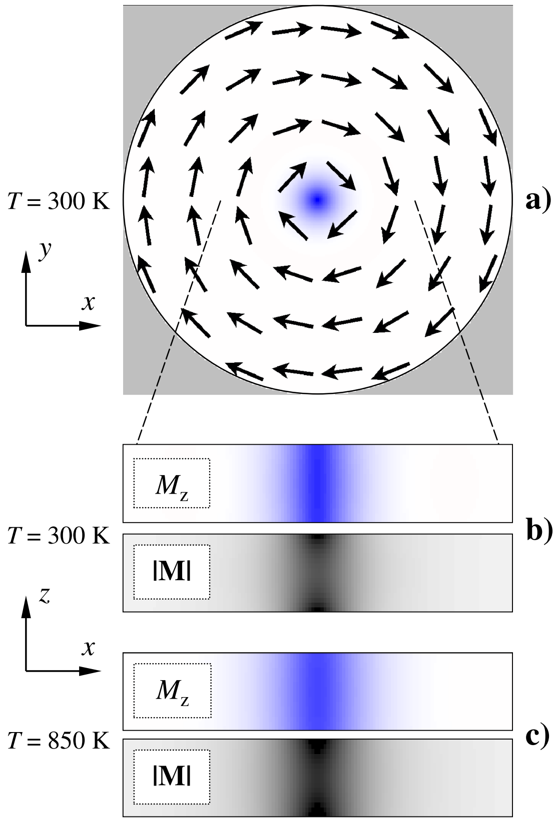

FIG. 1. (a) Top view of a circular permalloy island containing a vortex. Color coding depicts the out-of-plane magnetization component, M_z. (b) and (c) Blow-up of xz-cross sections through the center of the sample. In both cases, upper pictures have the same color coding as (a). Lower pictures present the magnetization magnitude—white means a value close to equilibrium, $M_e(T)$, while black is accordingly rescaled to present the *magnetization squeezing effect*: for $T = 300\,\text{K}$, black color represents $0.001\,M_e$, while for $T = 850\,\text{K}$, it represents $0.07\,M_e$.

Material parameters were chosen to mimic Py. The functions $M_e(T)$, $A(T)$, and $\chi_{\parallel}(T)$ have been obtained by rescaling the temperature dependence as obtained from atomistic modeling for FePt, similarly to Refs. 12–14. See the Appendix for the details. We have chosen $A(0) = 13 \times 10^{-12}\,\text{J/m}$, $M_e(0) = 0.86 \times 10^6\,\text{A/m}$, and a Curie temperature $T_C = 870$ K. We have neglected crystalline anisotropy effects. The damping constant α is 0.5 and we used a cuboid discretization cells with size $0.78125\,\text{nm} \times 0.78125\,\text{nm} \times 1.25\,\text{nm}$ (the origin of the coordinate system was in the center of our disk; see Fig. 1). The quality condition of performing reliable simulations was always fulfilled, as the parameter Δm_{max} introduced in Ref. 12 never exceeded the suggested limit of 0.5, being in our case always below 0.16.

Our object of interest was a ferromagnetic vortex in its steady state. For the chosen sample size, this is exactly the preferred state, for the whole considered temperature range (see the phase diagram in the Ref. 15).

III. RESULTS AND DISCUSSION

The upper part of the Fig. 1 shows a top view of our sample. The z-axis is a symmetry axis. The vortex core (VC) is clearly visible as region of dominating out-of-plane magnetization (colored in blue). In cross sections (b) and (c), we use the same color coding to show the z-component of the magnetization. We present also separately a gray-scaled color coding for the non-constant $|\mathbf{M}|$ value. Clearly, the magnetization magnitude is smaller inside the VC and we will call this effect "magnetization squeezing" in the following. If one notes the different color scaling for both temperatures, one can immediately recognize the dependence of this squeezing on temperature. This effect is related to the longitudinal susceptibility value but we will come to this point later. One can also see the weak dependence of presented phenomena on the z-position, more pronounced in the case of magnetization squeezing. This effect, called barrel-shape for the case of $T = 0$, was already found in the past and tackled analytically[16] and experimentally.[17] Therefore, all data presented in this paper were sampled once at the surface of the disk ($z = t/2$) and once in its central plane ($z = 0$).

To evaluate quantitatively the features shown in Fig. 1, we analyze the $M(\rho)$ and $M_z(\rho)$ dependence, where ρ is the radial distance from the VC axis, $\rho = \sqrt{x^2 + y^2}$. Fig. 2 shows M and M_z for cross sections along x and for two selected temperatures. There are a few theories that describe VC shape at zero temperature (see, for example, Refs. 18 and 19 for an overview). For our purposes, we have chosen the model of Feldtkeller, where the $M_z(\rho)$ profile is described by a Gaussian function[1]

$$M_z^{\text{fit}}(\rho, z) = M_{\min}(z) \exp\left(-\frac{\pi^2 \rho^2}{8\sigma_z^2(z)}\right). \tag{4}$$

Feldtkeller analyzed a $T = 0$ case, thus in his theory the prefactor in front of the exp-function was simply $M_e(T = 0)$.

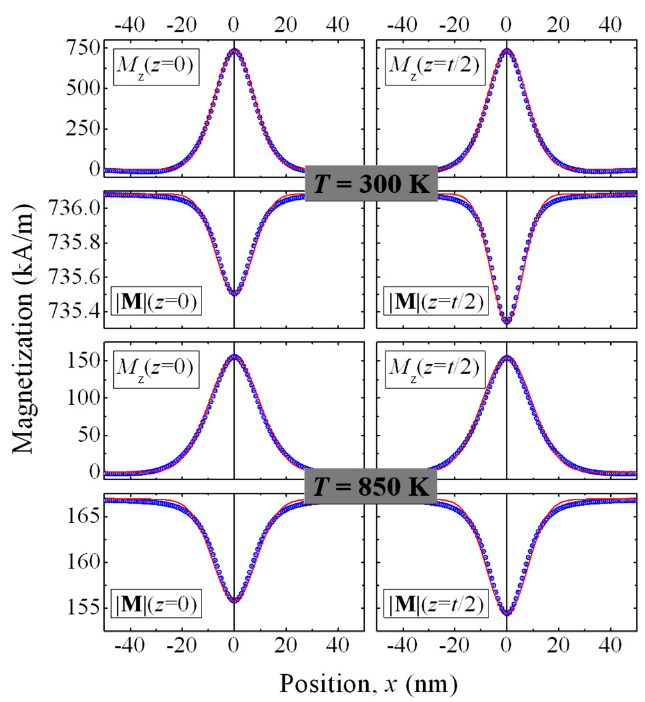

FIG. 2. Cross sections through the center of our sample containing the vortex core. For every temperature top figures show the M_z component, while bottom figures show the magnetization magnitude. We show separately results for the central plane ($z = 0$) and for the sample surface ($z = t/2$), for the two selected temperatures. Points show the results of our simulations while lines are fitted with a Gaussian function.

This is not the case for our study: because of the squeezing effect the peak magnetization value M_z in the center of the vortex is actually not M_e but a slightly smaller value that is determined separately for every above mentioned z-plane, which will be called $M_{min}(z)$ in the following. The parameter σ_z from Eq. (4) is the peak radius. Feldtkeller found an approximate solution for σ_z which we will call after him $R'_z(M_s, A)$, a function of the material parameters M_s and A (see Eqs. (3.9)–(3.11) in Ref. 1). In our case, the material parameters depend on temperature, thus the function $R'_z(T)$ will also depend on it. The parameter M_{min} was determined separately for every temperature considered by finding the minimum of the magnetization magnitude among all the cells in the given plane. The parameter σ_z was determined by a two-dimensional (in xy-plane) fitting of our simulation results with Eq. (4), separately for every z-plane (see Fig. 2 for results of this fitting procedure).

Fig. 2 suggests that the magnetization squeezing can also be described by a Gaussian profile. For consistency, we have fitted $|\mathbf{M}(\rho)|$ results using an analogous function,

$$M_{tot}^{fit}(\rho, z) = M_e - M_{min}(z) \exp\left(-\frac{\pi^2 \rho^2}{8\sigma_{tot}^2(z)}\right), \tag{5}$$

where again σ_{tot} is a fitting parameter and M_{min} was determined earlier. In all cases, the fitting was good and the fitting errors were smaller than the symbols representing the data in Fig. 4.

Fig. 3 shows the squeezed magnetization, M_{min}, for different simulated temperatures (points). The differences between $M_{min}(z=0)$ and $M_{min}(z=t/2)$ are so small that they cannot be shown in this figure. (These differences can be seen in Figs. 2 and 5, where vertical scale is fine.) For comparison, we show the equilibrium magnetization $M_e(T)$ as well (solid line). Our results do not deviate distinguishably from this curve, contrary to earlier reports investigating domain walls in FePt. The reason for this, we attribute to the different material considered in Ref. 6: FePt has a very strong crystalline anisotropy, so that the magnetization inside the domain wall is squeezed strongly by anisotropy interactions. Contrary to that case, here we have a soft material with negligible anisotropy. In our case, the squeezing is caused "only" by exchange interactions but we will come back to this point later.

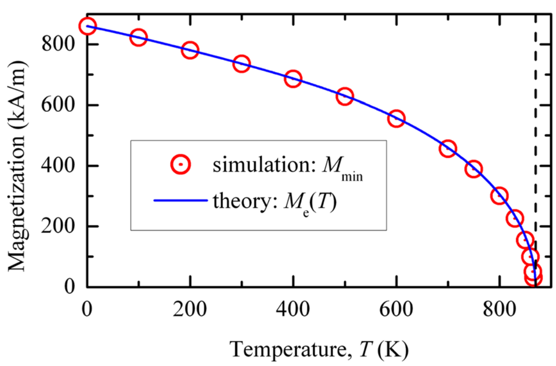

FIG. 3. Magnetization squeezing as a function of temperature (points). For comparison the equilibrium magnetization is plotted as solid line. The dashed line marks the Curie temperature.

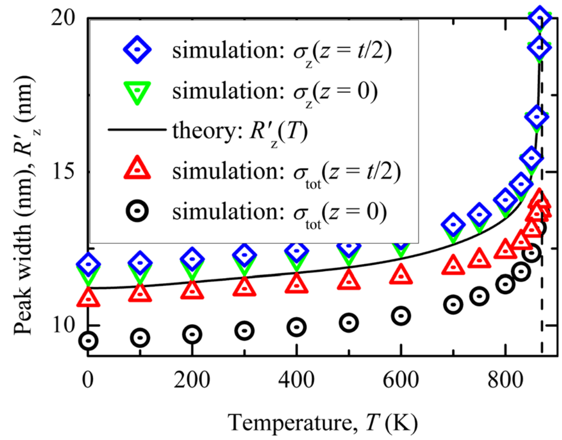

FIG. 4. Solid line: VC radius as predicted by Feldtkeller's theory.[1] Points (above the line): VC radius from our simulations. Points (below the line): "squeezing" radius of the Gaussian drop of the magnetization magnitude. The dashed line marks the Curie temperature.

Fig. 4 shows results of our fitting procedure for the peak radii σ_{tot} and σ_z (points). As noted before, the theory for the dependence $\sigma_z(T)$ can be concluded from Ref. 1 when the temperature dependence of the material parameters via functions $M_e(T)$ and $A(T)$ is taken into account. We show results of this theory in Fig. 4 as solid line. $R'_z(T)$ and $\sigma_z(T)$ match quit well, indicating that the magnetization squeezing effect in vortices in permalloy is weak and many properties of these vortices can be simply described by Feldtkeller's theory[1] when temperature-dependent functions $M_e(T)$ and $A(T)$ are used. The magnetization-drop radius, σ_{tot}, has also a similar temperature dependence. Contrary to σ_z, it is, however, smaller than $R'_z(T)$—an effect that can also be seen in Fig. 2. This difference is again rather small. More pronounced is the difference between $\sigma_{tot}(z=0)$ and $\sigma_{tot}(z=t/2)$—an effect that was also shown in Fig. 1. We attribute this difference to the influence of the demagnetization field.

As noted in Sec. II, the squeezing effect is controlled by the last element in Eq. (2), thus by the parallel susceptibility, $\chi_\parallel$. This dependence can be described with a simple theory. In soft magnetic samples, the exchange interactions are the dominating ones. Whether one considers the magnitude of the effective field, say in the middle of the VC, or the total energy (for the whole sample), for the samples evaluated here appropriate values for the exchange interactions are at least 6 times larger than for the dipolar interactions for all temperatures considered here. If one neglects $\mathbf{H}_d$ and sets $\mathbf{H}_{eff} = 0$—the condition for the stationary state in the LLB equation—one gets from Eq. (2)

$$\frac{2A}{\mu_0 M_e^2} \nabla^2 \mathbf{M} = \left(\frac{M^2}{M_e^2} - 1\right) \frac{\mathbf{M}}{2\chi_\parallel}. \tag{6}$$

Assuming a Gaussian shape of the VC and considering only the central axis of the vortex one obtains (if the VC points in the $+z$ direction)

$$\nabla^2 \mathbf{M}(0,0,z) = \left(0, 0, \frac{-\pi}{2\sigma_z^2} M_{min}(z)\right). \tag{7}$$

On the z-axis, the effective field has only a z-component. Combining both equations above yields

$$\frac{M_e - M_{min}(z)}{M_e} = 1 - \sqrt{1 - \frac{2\pi A}{\mu_0 M_e^2 \sigma_z(z)^2}\chi_\parallel}. \qquad (8)$$

As was shown before, $\sigma_z(z)$ can with good approximation be described by $R'_z(T)$. For the sample of interest, $\pi A/\mu_0 M_e^2 {R'_z}^2$ is a slowly varying monotonic function of temperature increasing roughly from 0.9 at $T=0$ to 1.8 at $98\% T_C$. Thus, the rhs of Eq. (8) is dominated by $\chi_\parallel$ and its strong temperature dependence. Up to $98\% T_C$, the argument of the square in Eq. (8) is larger than 0.9; thus it can be approximated with a Taylor expansion leading to the final result

$$\frac{M_e - M_{min}}{M_e} \approx \frac{\pi A}{\mu_0 M_e^2 {R'_z}^2}\chi_\parallel. \qquad (9)$$

The normalized squeezing effect, $(M_e - M_{min}(z))/M_e$, as found in our simulations is plotted with points in Fig. 5. For comparison, the theoretical dependence from Eq. (9) is shown as well (solid line). The line is drawn up to the mentioned limit of $98\% T_C$. Actually, for the sample of interest, the factor $\pi A/\mu_0 M_e^2 {R'_z}^2$ is so close to one and is so slowly changing with temperature (as compared to $\chi_\parallel(T)$) that the whole dependence can be further approximated by taking simply $\chi_\parallel$, presented as a dashed-dotted line in Fig. 5. The weak temperature dependence of the factor $\pi A/\mu_0 M_e^2 {R'_z}^2$ is caused by two reasons: First, the input functions for our simulations, $A(T)$ and $M_e(T)$, were obtained in such a way[20] that close to the Curie temperature $A(T)$ is roughly proportional to $M_e(T)^2$ (mean-field behavior). Second, the theory for $R'_z(A, M_e)$ actually uses A/M_e^2 rescaling—both for the input as for the output[1]—thus, if this fraction is quasi-constant then $R'_z(T)$ is quasi-constant as well.

Clearly, Eq. (9) underestimates the results of our simulations. This can be explained by the fact that only exchange interactions were included in our analysis. Dipolar interactions cause an additional squeezing of the magnetization so

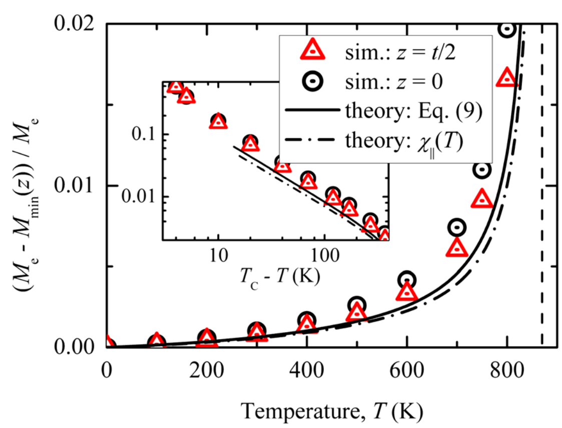

FIG. 5. Normalized magnetization squeezing effect in the vortex center, $(M_e - M_{min})/M_e$, as a function of the temperature (points). Lines represent approximated theory prediction. The dashed line marks the Curie temperature. Inset: logarithmic dependence close to the T_C.

that their inclusion would probably improve the agreement between theory and simulation data in Fig. 5. Another property characteristic for the demagnetization field is its inhomogeneity inside the VC. Considering the z-axis, $\mathbf{H}_d$ is smallest in the center of the sample increasing when the surface is approached. The influence of the demagnetizing field can be seen in Fig. 1, where the squeezing effect is larger close to the sample surfaces. This is also the reason why $\sigma_{tot}(z = t/2)$ is larger than $\sigma_{tot}(z = 0)$ and $M_{min}(z = t/2)$ is smaller than $M_{min}(z = 0)$ (see Figs. 2 and 4).

IV. SUMMARY

Vortex core properties have been evaluated by numerical simulations for a full range of temperatures for a material with permalloy-like properties. The LLB approach was used to include thermal effects. The results are well described with an appropriate theory, where we have used the approach of Feldtkeller[1] with material parameters which are related to appropriate functions entering the LLB equation. A magnetization squeezing effect, described already in the past, is weakly present in the vortex core, unless very close to the Curie temperature. We predict, however, stronger effects in materials with easy in-plane anisotropy where the magnetization squeezing in the VC would be additionally strengthened by anisotropy interactions. Evaluating squeezing in the vortex core is a first important step toward dynamical studies—like vortex core switching or oscillation.

ACKNOWLEDGMENTS

The work was supported by the *Kompetenznetz Funktionelle Nanostrukturen* funded by the Baden-Württemberg Stiftung.

APPENDIX: TEMPERATURE-DEPENDENT MATERIAL PARAMETERS

We rescaled material parameters for permalloy based on a set of material parameters computed originally for iron platinum—the equilibrium magnetization, $M_e^{FePt}(T)$, the exchange constant, $A^{FePt}(T)$, the longitudinal susceptibility, $\chi_\parallel^{FePt}(T)$, and the Curie temperature, T_C^{FePt}. The material parameters for FePt were calculated by atomistic spin model simulations. To obtain smooth temperature-dependent functions, these results were fitted with rational functions. Details about this procedure can be found in Ref. 20. Figures representing the atomistic results and the fitted functions can be found in Ref. 11. The temperature-dependent material parameters for permalloy were then obtained by a rescaling procedure

$$M_e(T) = \frac{M_e^{(0)}}{M_e^{FePt}(0)} M_e^{FePt}\left(\frac{T_c^{FePt}}{T_C}T\right),$$

$$A(T) = \frac{A^{(0)}}{A^{FePt}(0)} A^{FePt}\left(\frac{T_c^{FePt}}{T_C}T\right),$$

$$\chi_\parallel(T) = \frac{M_e^{(0)}}{M_e^{FePt}(0)} \chi_\parallel^{FePt}\left(\frac{T_c^{FePt}}{T_C}T\right).$$

Here, $M_e^{(0)}$ and $A^{(0)}$ are the assumed zero-temperature values for permalloy, in our case, respectively, $0.86 \times 10^6 \mathrm{A/m}$ and $13 \times 10^{-12} \mathrm{J/m}$.

[1]E. Feldtkeller and H. Thomas, Phys. Kondens. Mater. **4**, 8 (1965).
[2]K. Nakano, D. Chiba, N. Ohshima, S. Kasai, T. Sato, Y. Nakatani, K. Sekiguchi, K. Kobayashi, and T. Ono, Appl. Phys. Lett. **99**, 262505 (2011).
[3]R. Moriya, L. Thomas, M. Hayashi, Y. B. Bazaliy, C. Rettner, and S. S. P. Parkin, Nat. Phys. **4**, 368 (2008).
[4]B. C. Stipe, T. C. Strand, C. C. Poon, H. Balamane, T. D. Boone, J. A. Katine, J.-L. Li, V. Rawat, H. Nemoto, A. Hirotsune, O. Hellwig, R. Ruiz, E. Dobisz, D. S. Kercher, N. Robertson, T. R. Albrecht, and B. D. Terris, Nature Photon. **4**, 484 (2010).
[5]C. D. Stanciu, F. Hansteen, A. V. Kimel, A. Kirilyuk, A. Tsukamoto, A. Itoh, and Th. Rasing, Phys. Rev. Lett. **99**, 047601 (2007).
[6]D. Hinzke, N. Kazantseva, U. Nowak, O. N. Mryasov, P. Asselin, and R. W. Chantrell, Phys. Rev. B **77**, 094407 (2008).
[7]D. A. Garanin, Phys. Rev. B **55**, 3050 (1997).
[8]H. Kronmueller, in *Handbook of Magnetism and Advanced Magnetic Materials*, edited by H. Kronmueller and S. Parkin (Wiley-Interscience, Chichester, 2007), Vol. 2, pp. 703–741.
[9]We consider here only the case $T \leq T_C$.
[10]M. J. Donahue and D. G. Porter, "Oommf user's guide, release 1.2a4pre," Technical Report No. NISTIR 6376, National Institute of Standards and Technology, 1999.
[11]N. Kazantseva, D. Hinzke, U. Nowak, R. W. Chantrell, U. Atxitia, and O. Chubykalo-Fesenko, Phys. Rev. B **77**, 184428 (2008).
[12]K. Lebecki, D. Hinzke, O. Chubykalo-Fesenko, and U. Nowak, Phys. Rev. B **86**, 094409 (2012).
[13]C. Bunce, J. Wu, G. Ju, B. Lu, D. Hinzke, N. Kazantseva, U. Nowak, and R. W. Chantrell, Phys. Rev. B **81**, 174428 (2010).
[14]K. Vahaplar, A. M. Kalashnikova, A. V. Kimel, D. Hinzke, U. Nowak, R. Chantrell, A. Tsukamoto, A. Itoh, A. Kirilyuk, and Th. Rasing, Phys. Rev. Lett. **103**, 117201 (2009).
[15]K. L. Metlov and Y. P. Lee, Appl. Phys. Lett. **92**, 112506 (2008).
[16]A. Hubert and R. Schäfer, *Magnetic Domains* (Springer, Berlin, 1998).
[17]A. Thiaville, J. M. Garcia, R. Dittrich, J. Miltat, and T. Schrefl, Phys. Rev. B **67**, 094410 (2003).
[18]D. Altbir, J. Escrig, P. Landeros, F. S. Amaral, and M. Bahiana, Nanotechnology **18**, 485707 (2007).
[19]S. Gliga, "Ultrafast vortex core dynamics investigated by finite-element micromagnetic simulations," Ph.D. dissertation (Duisburg University, Duisburg, Germany, 2010).
[20]N. Kazantseva, "Dynamic response of the magnetisation to picosecond heat pulses," Ph.D. dissertation (University of York, York, UK, 2008).